

# NJC

Accepted Manuscript



This is an *Accepted Manuscript*, which has been through the Royal Society of Chemistry peer review process and has been accepted for publication.

*Accepted Manuscripts* are published online shortly after acceptance, before technical editing, formatting and proof reading. Using this free service, authors can make their results available to the community, in citable form, before we publish the edited article. We will replace this *Accepted Manuscript* with the edited and formatted *Advance Article* as soon as it is available.

You can find more information about *Accepted Manuscripts* in the [Information for Authors](#).

Please note that technical editing may introduce minor changes to the text and/or graphics, which may alter content. The journal's standard [Terms & Conditions](#) and the [Ethical guidelines](#) still apply. In no event shall the Royal Society of Chemistry be held responsible for any errors or omissions in this *Accepted Manuscript* or any consequences arising from the use of any information it contains.

## Polyvinyl alcohol/polysaccharides hydrogel graft materials for arsenic and heavy metal removal

Md. Najmul Kabir Chowdhury<sup>a,1</sup>, Ahmad Fauzi Ismail<sup>a</sup>, Mohammad Dalour Hossen Beg<sup>b</sup>, Gurumurthy Hegde<sup>c</sup>, and Rasool Jamshidi Gohari<sup>a</sup>

<sup>a</sup>Advanced Membrane Technology Research Center (AMTEC), Universiti Teknologi Malaysia, 81310 Johor Bahru, Johor, Malaysia

<sup>b</sup>Faculty of Chemical and Natural Resources Engineering, Universiti Malaysia Pahang, 26300, Gambang, Kuantan, Malaysia

<sup>c</sup>BMS R and D Centre, BMS College of Engineering, Basavanagudi, Bangalore 560019, India

### ABSTRACT

Water pollution caused from arsenic and some of the heavy metals have been reported widely all over the world. As one of them, the goal of this investigation is to develop different polysaccharides–polyvinyl alcohol (PVA) graft materials hydrogel for the removal of toxic and carcinogenic arsenic (As) species as well as series of heavy metals ( $Mn^{2+}$ ,  $Cr^{2+}$ ,  $Fe^{3+}$ ,  $Ni^{2+}$ ,  $Cu^{2+}$  and  $Pb^{2+}$ ) from contaminated water. Hydrogels were developed with PVA and PVA/polysaccharides (as blended materials) by using  $\gamma$ -ray irradiation technique and then characterized by Fourier transform infrared (FTIR) and gravimetric method. The absorbed dose of  $\gamma$ - radiation has been optimized to get good gel and some important physical parameters such as gel fraction, degree of swelling and water absorption kinetics of the synthesized hydrogels also been investigated. The optimum absorbed dose of 30kGy reveals the gel fraction of about 98% in the PVA/corn starch (CS) hydrogel. Developed hydrogels have the capability to make

---

\*Corresponding authors Email address: [chowdhurynajmul76@yahoo.com](mailto:chowdhurynajmul76@yahoo.com) (M. N. K. Chowdhury), [fauzi.ismail@gmail.com](mailto:fauzi.ismail@gmail.com) (A. F. Ismail), Telephone: +607-553 5592, Fax: +607-553 5925/553 5625.

chelate which are utilized for the removal of arsenic and heavy metals. Absorption of arsenic and heavy-metal ions from the respective aqueous solution by the chelating functionalized gels has been assessed by the Atomic Absorption Spectrophotometer (AAS). The calculated maximum amount of iron and arsenic removal capacity 37075 and 22112 mg/kg, respectively, have been found for the of PVA/CS hydrogel. It is also realized that polysaccharides (PS) analogues show affinity toward the metal ions to a considerable extent with the following order:  $\text{Fe}^{3+} > \text{Mn}^{2+} > \text{Cu}^{2+} > \text{etc.}$  The results obtained from this study indicate that the fictionalized hydrogels represent a good cheating tendency and suitable for water treatment.

**Key words:** hydrogel; polysaccharide; arsenic; heavy metal; chelating property; water treatment

## 1. Introduction

Around the globe, it is highly important to put the best efforts to combat the existing problems with the usage of technologies as well as to come up with new processes and modified materials to enable a more sustainable future, where the arsenic and heavy-metal free water is one of the potential requirements. Every day, 2 million tons of sewage, industrial and other effluents (with toxic species like heavy metals) are being discharged into aquatic systems and causing environmental problems.<sup>1-4</sup> Among the heavy metal releasing industries the major sources are automobiles, electroplating, ship-breaking, battery, leather tanning, fertilizer and pesticide; those are continuously discharging lead, copper and chromium pollutants.<sup>5-7</sup> Due to the necessity of industrial development it is not possible to ignore the usage of these toxic species in

chemical industries. However, among the industrial wastes most of them are well-known as toxic and carcinogenic. In addition, around the world more than 70 countries, natural water contains inorganic form of arsenic such as arsenite ( $\text{As}^{3+}$ ), where its degree of contamination reached in severe state and the impact of human life is at a great risk.<sup>8, 9</sup> To deal the mentioned complex relations, adoption of new and clean materials/green materials is undoubtedly welcomed by the experts of that related issues.<sup>10, 11, 12</sup>

To control the presence of these pollutants in wastewater, many techniques have been introduced for example adsorption, chemical precipitation, membrane filtration, ion exchange, coagulation, electrochemical treatment, flocculation, and flotation.<sup>13-15</sup> Among the techniques, adsorption is recurrently considered as one of the most appropriate techniques for the broad spectrum removal of pollutants since it is applicable for both organic and inorganic contaminants. Additionally, this technique is economical, convenient, effective and involved with less-troubles.<sup>16, 17</sup> The efficiency of pollutant adsorption predominantly governed by the type of adsorbents used and as an effective adsorbent for wastewater treatment gels are considered due to a wide range of applications.<sup>17-21</sup> Simply, gel is a polymeric network or non-fluid colloidal network, which can expand throughout the entire volume under an appropriate fluid. When water is considered as fluid, the developed gels will be referred as 'hydrogel'. The presence of porous network structure, hydrophilic functional groups, chelate formation capability, high water containing property, solute diffusion through the structure are intended them for the usage of wastewater treatment processes.<sup>18, 21, 22</sup> However, poor mechanical strength and the low water absorption kinetics sometimes hinder them from the practical application in wastewater treatment. In order to improve the quality of human life, mitigation of arsenic and heavy metals from drinking water has become a challenge to the researchers. Consequently, chelating functionalized polymeric

materials have been used with notable interests as adsorbent of the heavy metals and arsenic pollutants.<sup>23-25</sup> Besides; notable works can also be cited, where heavy-metal ions such as Hg, Pb, Ag and Cu were removed from water using different chelating resins.<sup>26-28</sup>

Although the use of some hydrogels for treating wastewater has been found in the open literature, however, the systematic use of a series of polysaccharides with PVA hydrogel along with a different route of development is still rarely reported. In the present study, radiation-induced grafting of PVA/polysaccharides (wheat-flour, rice-powder, maize-starch and corn-starch) hydrogels have been prepared and then characterized by gravimetric and FTIR techniques. The suitability of the prepared hydrogel for water treatment (especially, for the removal of arsenic and some heavy metals) has been reported here. The phenomena of gel formation by radiation technique and the adsorption of metals on hydrogels are also explained with some schematic presentations.

## **2. Materials and methods**

### *2.1. Materials*

Kappa-carrageenan was procured from Sigma Aldrich Ltd, Poole, UK and polyvinyl alcohol from BDH, Poole, England, Nutrient Agar (Oxoid, England) and Potato Dextrose Agar (Oxoid, England). Food grade polysaccharides like wheat-flour (WF) (faiza Tepung Gandum, Malaysia), rice-powder (RP) (TEPUNG BERAS, Malaysia), corn starch (CS) (KINGSFORD'S, Australia), and maize-starch (MS) (MAIZENA, Malaysia) was procured from the local market of Malaysia. All the materials and chemicals were used without further purification. Solutions of different metals, such as Cr, Cu, Fe, Mn, Ni and Pb were prepared from their respective nitrate

salts. 100 ppm arsenic (As) solution was prepared by diluting the sodium arsenite ( $\text{NaAsO}_2$ , 0.5M) standard solution.

## 2.2. Sample preparation

In hot deionized (DI) water, 7% (w/w) PVA solution was prepared first, which was used as a stock solution. In this stock solution polysaccharides (2.0%, w/w) added slowly with continuous stirring followed by the carrageenan (0.5%, w/w). Thereafter, the ingredients mixed solution was allowed to stand for overnight to ensure a homogenous mixture and then introduced in an autoclave at  $121^\circ\text{C}$  and 15 psi for 15 minutes. After functioning with an autoclave, the hot homogenous mixtures were transferred in disposable polyethylene terephthalate (PET) dishes, where it was allowed to cool and a bit settles condition. After that the materials in PET-dishes were sealed in polyethylene packs and exposed under gamma radiation; generated from a Co-60  $\gamma$ -ray source of energy 1.33 MeV. The exposed range of absorbed dose was 5–40 kGy. Due to the exposition under gamma radiation hydrogels were formed and used to determine various physico-chemical properties as well for water treatment.

## 2.3. FTIR characterization of polysaccharides and their graft materials with PVA

FTIR spectra of different polysaccharides and their graft materials were recorded over the frequency range  $4,000\text{--}500\text{ cm}^{-1}$  using a Thermo Scientific Model Smart Performer attenuated total reflectance (ATR) accessory of Ge crystal, attached to a Thermo Scientific spectrophotometer (Model: Nicolet Avatar-370) with a single bounce.

## 2.4. Gel fraction and optimization of absorbed dose

It is known that owing to the exposed radiation different degree of grafting and cross-linking have been possible in the mixture leading to the gel formation and gel fraction was estimated by gravimetric method. To do this, a fraction of the prepared hydrogel was dried in vacuum oven at 70 °C to a constant weight. As the gel was dried, a xerogel (gel where water content is zero) formed and the gel content (in that xerogel) was estimated by extracting its insoluble fraction. To extract, xerogels were put into the stainless steel net of 200 meshes after that immersed in hot DI water in an autoclave for 4 h at 121°C. The gel fraction was estimated with the help of the following relation:<sup>29, 30</sup>

$$G_f (\%) = \left( \frac{W_e}{W_0} \right) \times 100 \dots\dots\dots(1)$$

where,  $W_e, W_0$  and  $G_f$  are representing the weight of extracted gel after immersion, weights of xerogel and gel fraction, respectively. Moreover, dose optimization was reported from the maximum yield of gel fraction for each category of samples exposed under the dose range of 5–40 kGy of  $\gamma$ -ray. Four types of radiation grafted hydrogels were prepared and here-in-after abbreviated as PVA/WF, PVA/RP, PVA/CS, and PVA/MS.

### 2.5. Degree of swelling for hydrogel

For measuring the swelling performance of the cross-linked PVA/polysaccharides hydrogels, xerogels were immersed in DI water for 24 h at atmospheric condition. Thereafter, swollen samples were removed from DI water and the unabsorbed surface water was freed by thick and well-absorbing tissue paper and the target degree of swelling ( $D_s$ ) was measured by following Eq. (2):

$$X (\%) = \left( \frac{W_s - W_0}{W_0} \right) \times 100 \quad \dots\dots\dots(2)$$

Where,  $X=D_s$  and  $W_s$  is the weight of the gel in swollen state.

### 2.6. Water absorption kinetics

To study the water absorption behavior of the prepared hydrogels rectangular shaped specimens were taken where the dimensions (length  $\times$  wide) are 30  $\times$  28 mm. The test of water absorption was done as per standard test method ASTM D5703.<sup>31</sup> The initial weight ( $W_0$ ) of the specimen was measured after oven drying at 70 °C for 24 h. After the withdrawal of the specimen from the water bath/tank, surface water was removed by following the same technique as stated above and weighed ( $W_s$ ) by a calibrated analytical balance. The water uptake percentage at any particular time ( $t$ ) of immersion is expressed as  $W_t (X)$  which is calculated by following the Eq. (2). The immersion was continued until the saturation with water molecules. All of the used results were taken from the average value of three samples for each category of hydrogel materials and  $W_s$  is the weight of the gel after immersion in water.

According to the Fick's law, the concentration gradient is the driving force for the diffusion of water and the quantity of diffusion is a function of time. Usually, the prediction of Fick's law is satisfactorily valid for the water absorption behavior. In the case of this prediction, the absorbed water mass increases linearly with the square root of time, afterwards slows down up to an equilibrium plateau:<sup>31</sup>

$$D = \pi \left[ \frac{d}{4M_m} \right]^2 \left[ \frac{M_2 - M_1}{\sqrt{t_2} - \sqrt{t_1}} \right]^2 \quad (3)$$



Where  $M_m$  is the maximum moisture content,  $d$  is the thickness of the sample,  $t_1$  and  $t_2$  are the selected points in the initial linear portion,  $M_1$  and  $M_2$  are the respective moisture content.

### 2.7. Test of sterility for hydrogels

The sterility tests of prepared hydrogels were performed by the standard plate count method and during the test both spread and poured plates were used.<sup>29</sup> Nutrient Agar and Potato Dextrose Agar were used for bacterial and fungal count, respectively. Specific weight of hydrogel was divided into pieces aseptically and immersed in physiological saline/phosphate buffered saline. Thereafter, 0.1 mL suspension was spread onto the previously solidified media and 0.1 mL suspension was poured in a sterile petri - dish. All the cases, at least three replicas of each specimen were made for testing. The testing plates were then incubated at 37 and 30°C for bacteria and fungus, respectively. Every day the plates were checked for any visible growth and which was continued up to 21 days and when no visible growth observed up to 21st day, the hydrogel sample was then reported as sterile material.

### 2.8. Performance towards the metal and arsenic removal

The radiation processed chelating functionalized hydrogels were dipped in different metal ion standard solutions, including  $\text{Cr}^{+3}$ ,  $\text{Mn}^{+2}$ ,  $\text{Fe}^{+3}$ ,  $\text{Ni}^{+2}$ ,  $\text{Cu}^{+2}$  and  $\text{Pb}^{+2}$ . The concentration of the standard solution was 100 ppm and the pH was as neutral. To study the removal performance of the prepared PVA/polysaccharides hydrogels, 0.5g of them was immersed indifferent metal ion solutions (200 mL) individually for 12h with continuous shaking (500 rpm). The metal ion concentrations in the initial solution and the solution obtained after removal was determined by

AAS technique. The performance of the metal ion removal by the prepared hydrogel was determined by following the Eq.(4).<sup>8</sup>

$$U_m = \frac{(C_0 - C)V}{W} \dots \dots \dots (4)$$

Where,  $U_m$  is the metal uptake,  $C_o$  and  $C$  represent the concentrations of the metal solution before and after the usage of hydrogels,  $V$  is the volume of solution, and  $W$  is the weight of the hydrogels used for removal performance measurement.

### 2.9. Performance of re-use

PVA/polysaccharides chelated hydrogels (0.5 g) were shaking continuously with HCl (100 mL, 2 M) at 50 °C for 2 h to desorb the metal ions. Thereafter, the hydrogel was neutralized with dilute NaOH, washed with deionized water and again subjected to chelation processes. In the same way, to desorb the arsenic species 2 M, NaOH solution (100 mL) was used with continuous shaking after that neutralized by diluting HCl solution. To measure the desorption ratio ( $D_r$ , %) the following equation (5) was used.<sup>3</sup>

$$D_r = \left( \frac{\text{Quantity of adsorbed As}^{3+} \text{ species}}{\text{Quantity of desorbed As}^{3+} \text{ species}} \right) \times 100 \quad (5)$$

## 3. Results and Discussion

### 3.1. Gel fraction and optimization of absorbed dose

The effect of absorbed dose ( $\gamma$ -radiation) on the gel fraction in different polysaccharides/PVA hydrogels is shown in **Fig.1**, where the gel fraction versus absorbed dose plot indicates that up to 10 kGy the  $G_f$  was very low in all cases; however a rapid rising tendency

was observed from 15 to 20 kGy doses thereafter, it was shown almost level-off tendency and continued up to 35kGy. In contrast, at the used high dose (40 kGy), it was decreased slightly which might be due to the degradation of the PVA/polysaccharides hydrogels.

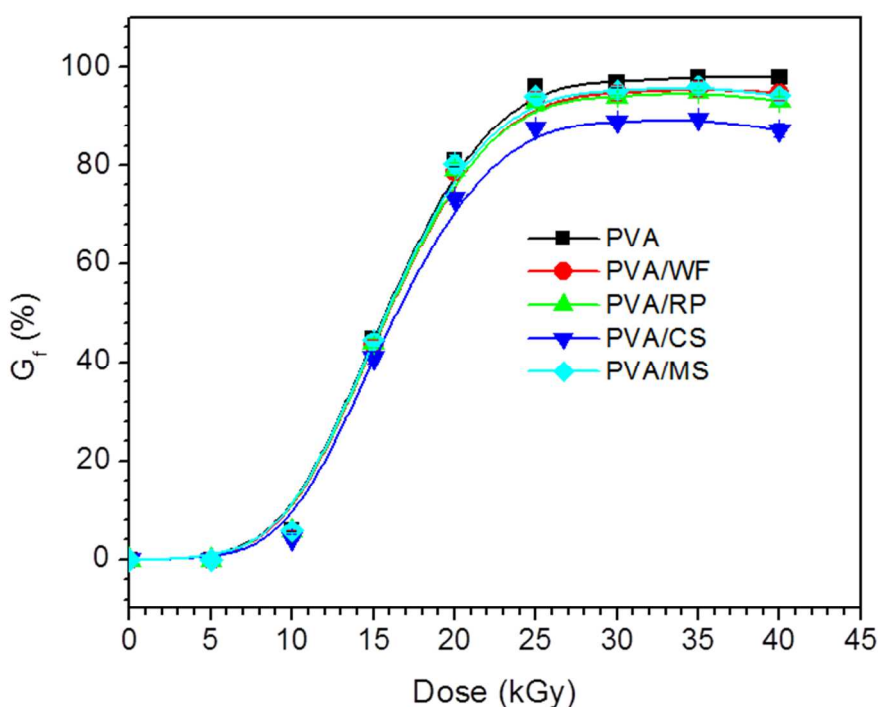
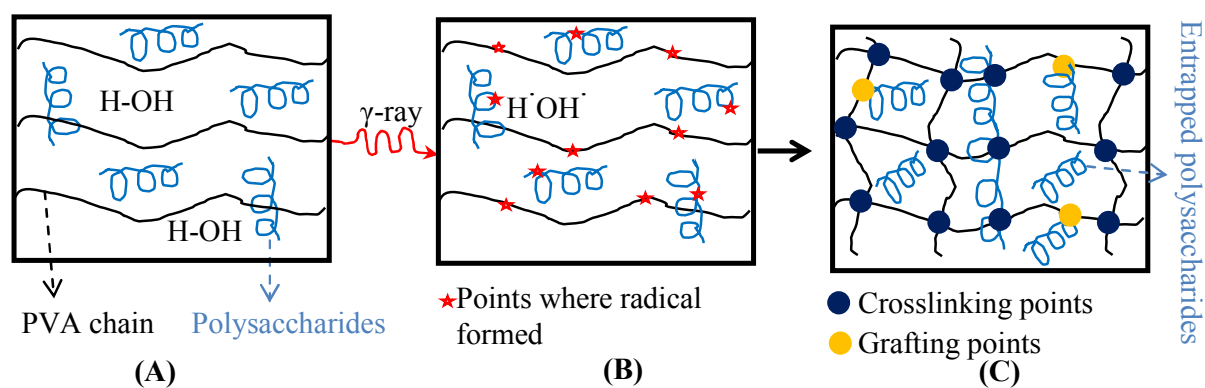


**Fig. 1:** Gel fraction ( $G_f$ ) of hydrogels with absorbed dose

Among the individual hydrogels, the decreasing order of  $G_f$  was: PVA/CS < PVA/WF < PVA/RP < PVA/MS < PVA. The observed result indicates that due to the addition of polysaccharides  $G_f$  value was decreased, and the trend of this decreasing was varied with the type of polysaccharides also. Among the used polysaccharides, lowest  $G_f$  observed for CS and highest for MS based hydrogels, signifying that increasing content of starch in PVA/polysaccharide blend systems retarded the  $G_f$  of hydrogel, which is consistent with the study performed by Zhai et al. (2002).<sup>30</sup> Basically, when aqueous solutions of PVA and

polysaccharides was exposed under ionizing radiation (**Scheme 1 (A)**), hydroxyl free radicals were formed in the system (**Scheme 1 (B)**) and this highly reactive species is able to form a gel structure through crosslinking and grafting (**Scheme 1 (C)**).<sup>29</sup> Initially, the hydroxyl radicals could propagate the formation of PVA and starch radicals (**Scheme 1 (B)**) and the generated PVA radicals interact easily with other PVA radicals to form cross-linked PVA networks. However, the crosslinking possibility of starch macro-radical to macro-radical was very low, rather due to irradiation starch may degrade easily.<sup>30</sup> In addition to, starch radicals interact with PVA radicals to propagate the graft reaction (**Scheme 1 (C)**).



**Scheme 1:** Effect of radiation on PVA and polysaccharides in water

It is mentioned that during irradiation PVA can cross-linked easily and sometimes this degree of cross-linking may be over the expectations, leading to the prepared hydrogels may show brittleness and poor mechanical strength. This can be circumvented with the addition of different types of polysaccharide which may be entrapped (**Scheme1 (C)**) through physico-chemical bonding in the gel network structure and can reduce the crosslinking density of the base polymer

and they become part of the hydrogel. To measure  $G_f$  (ratio of the weight of extracted and un-extracted gels) through extraction the entrapped polysaccharides can be removed from the hydrogels but the grafted (attachment through chemical bonding) polysaccharides exist in the hydrogel system.

### 3.2. FTIR study for polysaccharides and their graft formation

The infrared spectra (as shown in **Fig. 2(a)**) of different polysaccharides exhibited almost identical bands, because these bands have been originated mainly from the vibrational modes of starch components amylose and amylopectin. The most significant differences between the infrared spectra of different nonirradiated polysaccharides (starch sources) were observed in the O–H stretching regions of water molecule ( $3000\text{--}3600\text{ cm}^{-1}$ ), possibly due to differences in water content. The FTIR absorption band assignments are presented in **Table 1**.

**Table 1:** Band assignments for FTIR spectra of polysaccharides

Absorption at ( $\text{cm}^{-1}$ )	Assigned for
3000–3600	O–H stretching <sup>32</sup>
2800–3000	CH <sub>2</sub> deformation <sup>29, 33, 34</sup>
1644	Water adsorbed in the amorphous regions of starch <sup>32</sup>
1415	CH <sub>2</sub> bending, C–O–O stretch <sup>32</sup>
1344	C–O–H bending, CH <sub>2</sub> twisting <sup>32</sup>
1242	CH <sub>2</sub> OH (side chain) related mode <sup>32</sup>
1163	C–O, C–C stretching <sup>32</sup>

1127	C–O–H bending <sup>32</sup>
1067	C(1)–H bending <sup>32</sup>
930	skeletal mode vibrations of $\alpha$ -1,4 glycosidic linkage (C–O–C) <sup>32</sup>
860	C(1)–H, CH <sub>2</sub> deformation <sup>32</sup>
764	C–C stretching <sup>32</sup>
650	skeletal modes of pyranose ring <sup>32</sup>
568	
535	
518	

---

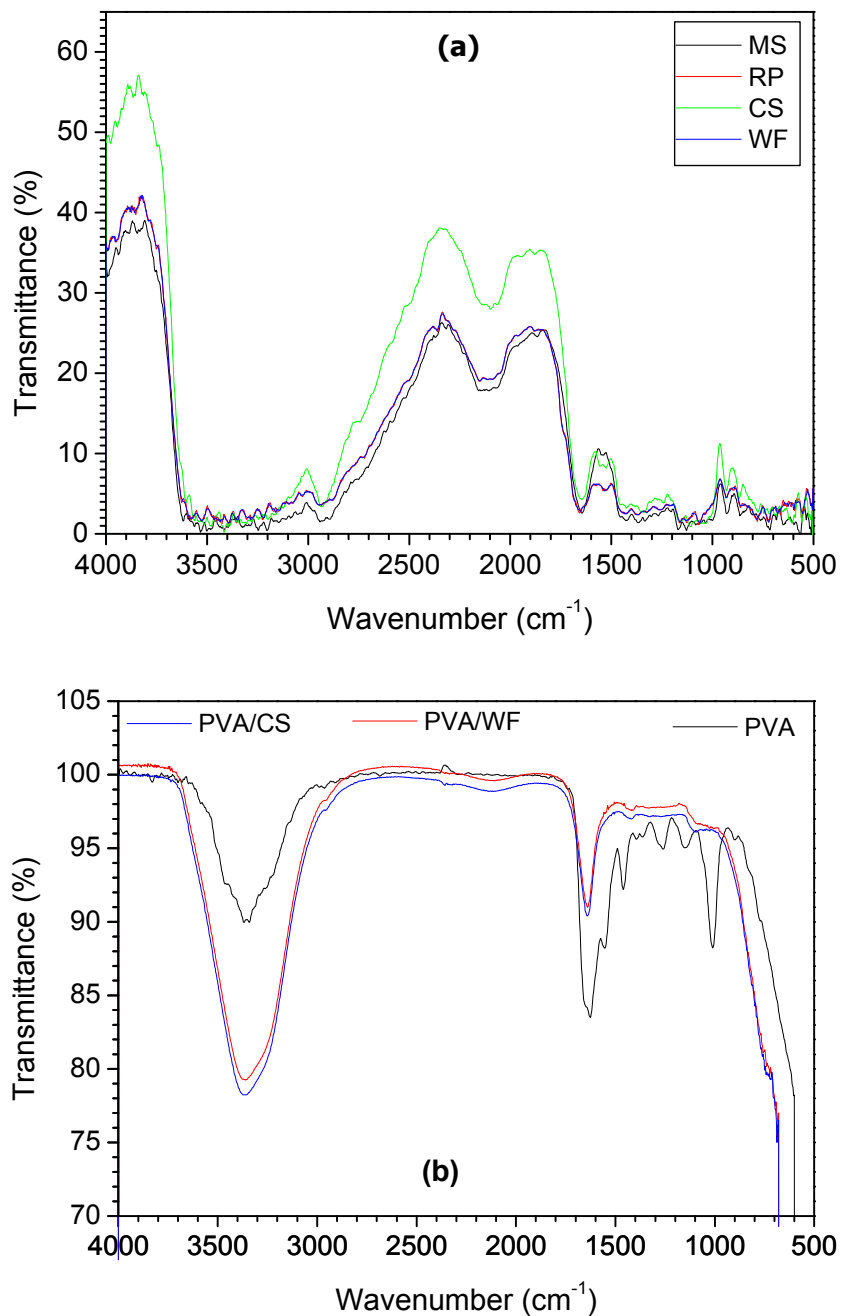


**Fig. 2:** FTIR spectra of (a) different polysaccharides, and (b) their graft materials with PVA

Investigation of the spectra (**Fig. 2 (a)**) has been done in four main regions which may help in successive interpretation and characterization of the key bands. These regions were categorized

as follows: 3000–3600  $\text{cm}^{-1}$  (O–H stretch region), 2800–3000  $\text{cm}^{-1}$  (C–H stretch region), 800–1500  $\text{cm}^{-1}$  (the fingerprint region), and below 800  $\text{cm}^{-1}$ .

Spectral analysis confirms the presence of O–H and C–H stretching absorption for the polysaccharides and their graft materials. The observed peak in the region 3000–3600  $\text{cm}^{-1}$  in the FTIR spectra (**Fig. 2(a)**) indicates the O–H stretching mode of polysaccharides and the stretching vibration peak in the 2800–3000  $\text{cm}^{-1}$  region confirms the presence of C–H group. In this range, the spectrum to spectrum intensity change may indicate the variations of the quantity of amylose and amylopectin present in the polysaccharides. For instance, CS has 28% amylose, whereas MS has quite lower than this amylose content<sup>32</sup>.

The observed absorption frequency at 1644  $\text{cm}^{-1}$  (in **Fig. 2(a)**) was ascribed to the adsorbed water in the amorphous region of starch moieties of the polysaccharides. Since this characteristic peak is related to the crystallinity of starch/polysaccharides, the variations of peak pattern, intensity and position of this peak for different polysaccharides indicate the crystallinity differences of different polysaccharide samples.<sup>32</sup> In this study, it is also observed that MS presented sharpest bands at ~1644  $\text{cm}^{-1}$  than those of other polysaccharides, which is possibly due to the variances of the crystal polymorph of the starch exist in MS. A broad infrared peak at 1632  $\text{cm}^{-1}$  could be assigned for the adsorbed water in the amorphous parts of the polysaccharides. With increasing the crystallinity of starch (available in polysaccharides) the band at 1632  $\text{cm}^{-1}$  becomes weaker in the infrared absorption spectra, and for most crystalline cellulose, this band was barely observed<sup>32</sup>. This finding satisfies the hypothesis that the band at 1632  $\text{cm}^{-1}$  is a consequence of the vibrations of water molecules which is adsorbed in the non-crystalline region of polysaccharides.



In the spectra, the region 1500–800 $\text{cm}^{-1}$  (finger print region) displayed highly overlapping and complex nature that experiences the exact band assignment difficult<sup>32</sup>. The FTIR spectra of polysaccharides (largely amylose and amylopectin) in finger print region mainly exhibit for the vibrational state of glucose monomer<sup>32, 35</sup>. As a result, the assignment of wavenumbers for the respective monomers can give us the information about the assignment of polysaccharides. As in the spectral region below 1500  $\text{cm}^{-1}$  designates the vibrational bands of glucose molecules, which are dominating in the FTIR spectra and so the polysaccharides exhibit very similar spectral features in this region.

Carbon and hydrogen atoms containing groups show the vibrational (bending and deformation) bands in the region 1500–1300  $\text{cm}^{-1}$ <sup>32, 35</sup>. The band at 1344  $\text{cm}^{-1}$  could be ascribed for  $\text{CH}_2$  bending modes, the absorption band at 1242  $\text{cm}^{-1}$  was assigned for the  $\text{CH}_2\text{OH}$  related mode as well as the C–O–H deformation mode. The peak at 1163  $\text{cm}^{-1}$  was believed because of the coupling modes of C–O and C–C stretching, and the band at 1127  $\text{cm}^{-1}$  could be attributed to the C–O–H bending modes. In the spectra of starch containing polysaccharides, very subtle changes in the peak location and intensity of the glycosidic linkage band occurred. The possibility of the change in the location can be attributed due to the presence of  $\alpha$ -1,6-linkage of the amylopectin that shifts the band to higher wavenumbers with varying the polysaccharides. The vibrations initiating from the C–O–C of  $\alpha$ -1,4-glycosidic linkages could be observed in the vicinity of 930  $\text{cm}^{-1}$  in polysaccharides<sup>32, 36</sup>. Glycosidic linkage is defined as the bonding between the first carbon atoms of a glucose unit with the fourth carbon atom of the other glucose unit via an oxygen atom (C1–O–C4). Stretching vibrations of (C1–O) and (C4–O) of the glycosidic linkage could be detected by vibrational spectroscopic methods, and the region 950–900  $\text{cm}^{-1}$  assigned for the glycosidic-linkage related vibrational modes.

Infrared spectra of polysaccharides exhibited complex vibrational modes at low wavenumbers (below  $800\text{ cm}^{-1}$ ) due to the skeletal mode vibrations of the glucose pyranose ring<sup>36</sup>. In this study, major bands at  $650$  and  $568\text{ cm}^{-1}$  and minor bands at  $535$  and  $518\text{ cm}^{-1}$  in the spectra (**Fig. 2 (a)**) of polysaccharides were attributed to the skeletal modes of the pyranose ring.

On the other hand, in **Fig. 2 (b)** the spectra of hydrogels are shown and for simplicity the spectra of PVA/RP and PVA/MS has not been presented here and the pattern of those spectra was similar of the presented spectra of PVA/WF except the intensity. During the process of gel formation, there is a possibility to cause substantial changes in both the chemical and physical nature of granular polysaccharides due to the rearrangement of intra and inter molecular hydrogen bonding between water and starch moieties of polysaccharides. The C–H stretch region  $2800\text{--}3000\text{ cm}^{-1}$  showed a dramatic intensity decrease upon irradiation. However, a slight broadening was detected in the O–H stretch ( $3000\text{--}3600\text{ cm}^{-1}$ ) region due to the uptake of water by the polysaccharides, which is also observed in elsewhere.

In this study, the effects of  $\gamma$ -irradiation on PVA/polysaccharides hydrogels were evaluated at the molecular level by means of FTIR spectroscopy. **Fig. 2 (b)** shows the FTIR spectra of different hydrogels at 30-kGy-irradiated forms for visual evaluation of the  $\gamma$ -irradiation effect. The spectral changes caused by  $\gamma$ -radiation exposure were apparent in the O–H stretch ( $3000\text{--}3600\text{ cm}^{-1}$ ), C–H stretch ( $2800\text{--}3000\text{ cm}^{-1}$ ), and bending mode of water ( $1600\text{--}1800\text{ cm}^{-1}$ ). Especially, in **Fig. 2 (b)** the absorption peaks for O–H observed at high field (at  $3369\text{ cm}^{-1}$ ) for PVA hydrogel, whereas for PVA/CS hydrogel it was at  $3349\text{ cm}^{-1}$  and the shifting of this peak at down field is an indication of graft material formation. The changes visually detected in the C–H stretch region of the spectra (**Fig. 2 (b)**) of irradiated PVA/polysaccharides hydrogels are in good agreement with the literature. The most prominent ionizing radiation damage to carbohydrates is

the liberation of a hydrogen atom from any C–H bond through the attack of hydroxyl radicals<sup>32</sup>. Because of this, the C–H stretch region can also be screened to develop the graft materials. Moreover, in the spectra of PVA hydrogel some peaks (at 1259.95, 1152.12, 1011.45, 900.62, 833.37 and 777.96  $\text{cm}^{-1}$ ), whereas these peaks was not observed in the spectra of PVA/polysaccharides hydrogels. These findings indicate the formation of PVA/polysaccharides hydrogels graft materials.

The breaking of chemical bonds by irradiation is called radiolysis that yields unstable, reactive agents, which are subsequently converted to stable end products. Because water is the most abundant molecule in polysaccharides hydrogels, reactions of water radiolysis products, namely, hydroxyl radicals, free hydrogen atoms, and aqueous electrons (i.e., solvated electrons), with constituents of food are predominant in the determination of radiation-induced chemical changes. The free radicals formed upon radiolysis of water trigger radiation-induced modifications in polysaccharide structure through very complicated free-radical reactions<sup>35</sup>. Water is not only being consumed by the radiolysis but is also formed as a reaction product through the interaction of free radicals with various molecules present with PVA and polysaccharides.

### 3.3. Degree of swelling

One of the general characteristics of hydrogel is its capacity to absorb and uphold substantial mass of solvent. In this study, the term degree of swelling ( $D_s$ ) indicates the mass of absorbed water by 1.0 g of xerogel. Swelling behavior can be explained from the structure of the polysaccharides and the radiation effect on the PVA/polysaccharides system. The used polysaccharides contain polar –O–H functional group (ionic groups); carrageenan is also bearing sulfate moieties. Due to irradiation, polysaccharide molecules break down<sup>37</sup> and then the small segment of polysaccharides with different functional groups and localized charges are entrapped

into the network structure of hydrogel, which are influencing the swelling performances of the hydrogels.<sup>38</sup> Especially, ionic groups have a tendency to increase the number of counter ions inside the gel, resulting to make an additional osmotic pressure and ultimately swell the gel structure.<sup>39</sup> The degree of swelling of PVA/polysaccharides hydrogels is shown in **Fig.3**. From this Figure, it is clear that  $D_s$  varied with the variation of polysaccharides. The obtained order of swelling: PVA/CS>PVA/WF>PVA/RP>PVA/MS>PVA and which is reverse order of the obtained  $G_f$ . This variation is logical, as the CS contains the maximum amount of starch than others and for absorbing water, in PVA/CS hydrogel system maximum number of available –O–H groups were present than others, leading to the absorption of uppermost quantities of water. In contrast, PVA hydrogel showed lowest  $D_s$  compare to the blended hydrogels, this is because of the higher degree of crosslinking and least number of available–O–H group in PVA hydrogel.

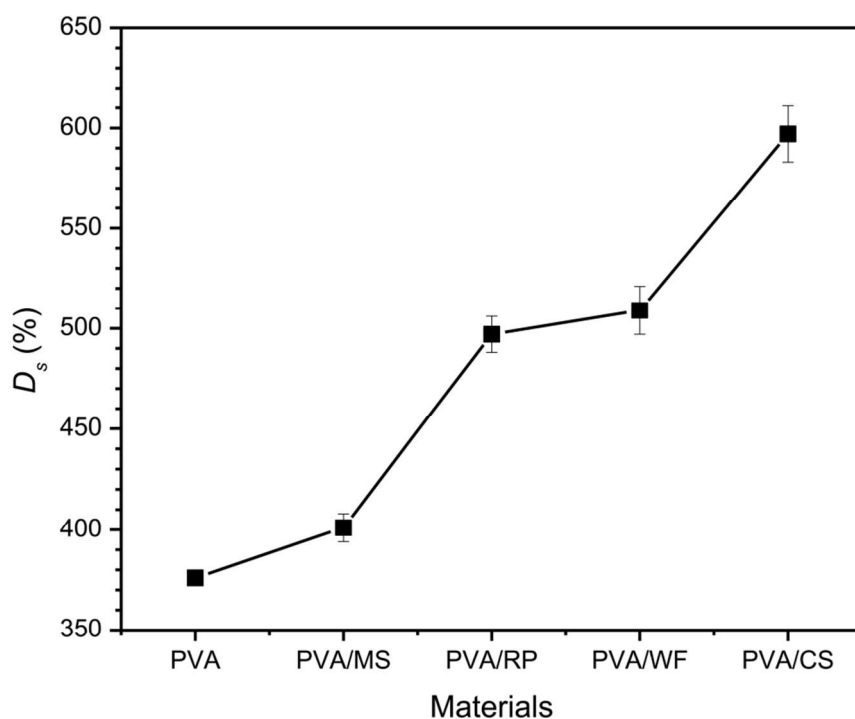


**Fig. 3:** Degree of swelling ( $D_s$ ) of different hydrogels

### 3.4. Water absorption kinetics

Considering the field of applications in some cases the absorption kinetics of hydrogel is highly important. **Fig. 4** shows the typical absorption curves of PVA and PVA/polysaccharides hydrogels where weight gain as a function of exposure time in water at room temperature. In each case, it is observed that at the beginning of the water absorption process it is sharp thereafter leveled off for some range of time where it reaches equilibrium. In this study, it is thought that the change of weight gain for all samples it is highly related with a typical Fickian diffusion behavior. Comparatively, PVA/polysaccharides hydrogels show higher water absorption performance than sans-polysaccharide PVA hydrogel. However, due to the using of polysaccharides in hydrogels the water absorption rate is increased. Overall, it is apparent that among the PVA/polysaccharides hydrogel systems, maximum uptake of water was done by CS polysaccharide (since it contained maximum starch or amylose). As shown ((**Scheme 1** (a, b)), the modification through radiation can reduce the free hydroxyl group in the chain of the base polymer; however, polysaccharides may break-down, can entrapped in the cross-linked structure of PVA, may grafted with PVA strand and can increases the hydrophilicity (through the starch content of polysaccharides) of the hydrogel system, thus increasing the water absorption.

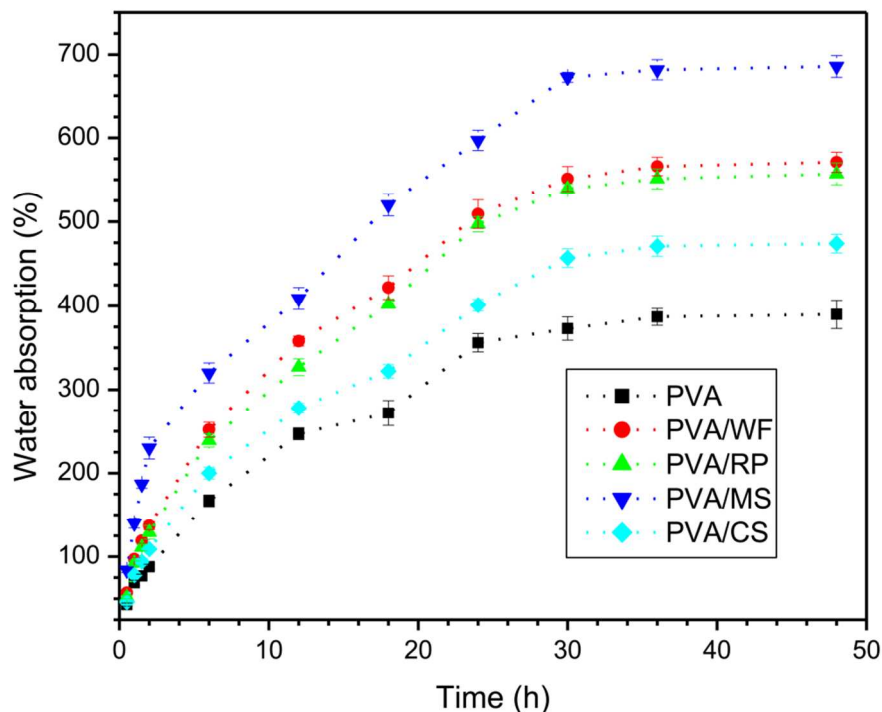


**Fig. 4:** Water absorption performances of different hydrogels

The result of water uptake is in accordance with  $D_s$  (section 3.2) and some previous works.<sup>29, 31, 40</sup> However, for this type of materials water absorption is substantially varied on polysaccharides type and loading, temperature, permeability of polysaccharides, orientation, surface protection, diffusivity, area of the exposed surfaces, etc.<sup>30, 31, 41</sup> Das et al.(2000) reported that initially, water molecules saturate the cell wall of the polysaccharides, and then, occupies the void spaces of the polysaccharides and cross-linked PVA systems.<sup>42</sup> **Table 2** summarizes the water absorption parameters such as diffusion coefficient ( $D$ ) and the moisture content at saturation point ( $M_m$ ). On the basis of  $D$  values of the composites, it is also possible to say that the polysaccharide blended PVA hydrogels have a better affinity towards water absorption than those of without polysaccharide PVA hydrogel. Polysaccharide blended PVA hydrogels showed the higher  $D$

value, which might also indicate higher amylose content from the entrapped polysaccharide in the blend system where that amylose facilitates more pathways for water uptake and to increase the diffusion into the hydrogels. The rate of diffusional process decreases with increasing the gel fraction, since better gel fraction indicates a higher degree of crosslinking and deficient gaps in the cross-linked system, can increase the crystallinity and hydrophobicity of matrix, which are leading to decrease the water absorption of that polymeric matrix. Moreover, higher crosslinking can cause to the decreasing of  $M_m$ .<sup>41</sup> Thus,  $M_m$  values of PVA were least than that of blended hydrogels.

**Table 2:** Diffusion coefficient and moisture contents of hydrogels

Materials	$D (\times 10^{-16}) \text{ m}^2 \text{ s}^{-1}$	$M_m(\%)$ at 48 h
PVA	3.24±0.03	390±9.61
PVA/MS	4.22±0.04	557±11.59
PVA/RP	5.72±0.13	571±9.96
PVA/WF	6.62±0.19	574±8.43
PVA/CS	23.46±0.90	686±12.17

### 3.5. Test of sterility

**Table 3** shows the densities of microorganisms in both non-irradiated and irradiated samples. From this table, it is clear that all of the non-irradiated samples are contaminated by bacteria only and this contamination, also varied with the type of polysaccharides where the most contaminated sample is PVA/CS system and the least one is PVA. However, all of the irradiated samples are entirely free from both types of microorganisms like bacteria and fungi, which is

very rational that due to exposed gamma radiation the present microorganisms in the sealed packs of hydrogels will be expired and the resultant samples will be sterile. This finding indicates that the prepared hydrogel can be usable safely.

**Table 3:** Microbial densities found in the prepared hydrogels

Materials	Microorganisms (*cfu/gm)			
	Bacteria		Fungi	
	Before	After	Before	After
	irradiation	irradiation	irradiation	irradiation
PVA	$2.4 \times 10^2$	Nil	Nil	Nil
PVA/MS	$3.4 \times 10^3$	Nil	Nil	Nil
PVA/RP	$5.6 \times 10^3$	Nil	Nil	Nil
PVA/WF	$7.3 \times 10^3$	Nil	Nil	Nil
PVA/CS	$8.1 \times 10^3$	Nil	Nil	Nil

\*cfu: colony forming unit

### 3.6. Performance towards the metals and arsenic removal

The metal uptake by different PVA hydrogels is shown in **Fig. 5 (a)** and **(b)**. The PVA/polysaccharides blended hydrogels exhibited a higher adsorption tendency towards  $\text{Cr}^{3+}$ ,  $\text{Mn}^{2+}$  and  $\text{Fe}^{3+}$  ions than  $\text{Ni}^{2+}$  and  $\text{Cu}^{2+}$  ions. The  $\text{Pb}^{2+}$  ion adsorption capacity by all of the prepared hydrogels is comparatively low.



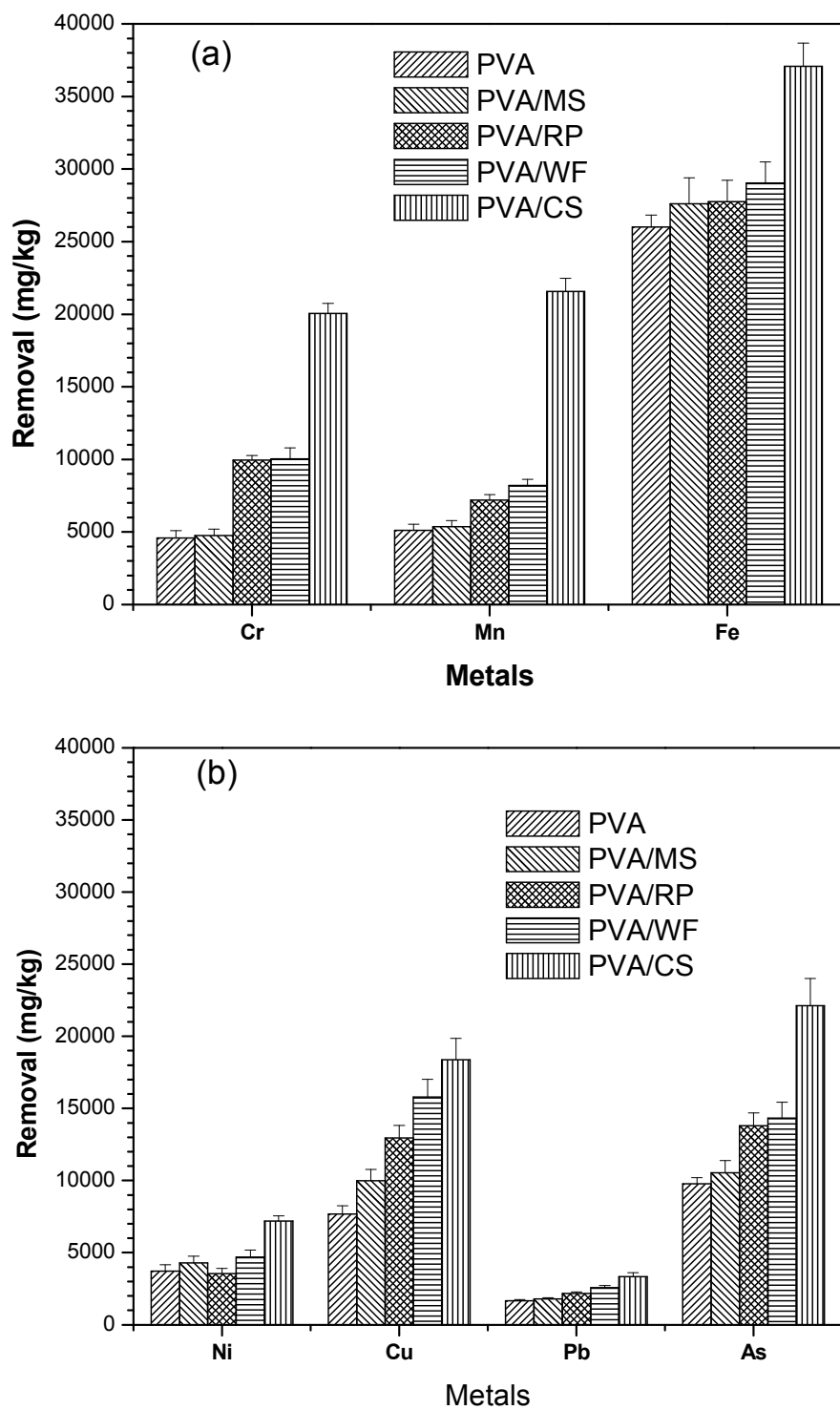
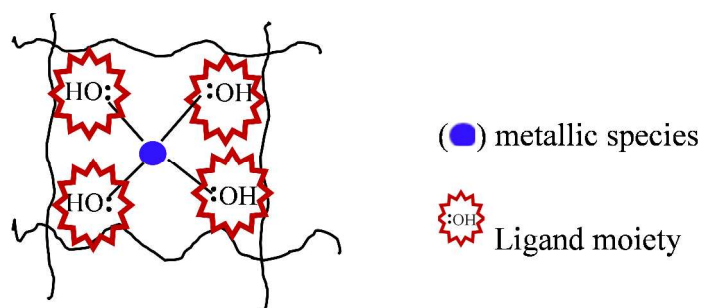


Fig. 5: Removal of heavy metal and arsenic by hydrogels

Thus, the chelating hydrogels showed different affinities towards the metal ions' adsorption. The adsorption of metal ions on the prepared hydro gels having oxygen donor (hard base) atoms followed the order of  $\text{Fe}^{3+} > \text{Mn}^{2+} > \text{Cr}^{3+} > \text{Cu}^{2+}$ . The consequences could be explained on the basis of availability of ligand site, charge and size of metal ion and the structure of chelate.

The reaction for common ligands (basically  $-\text{O}-\text{H}$  functional group of starch and PVA) with dissimilar metal ions or metal complexes generally exhibits various coordination structures. It is reported that  $\text{Cu}^{2+}$  can commonly be 4-or 6-coordinated and may exist in several geometries (as shown in **Scheme 2**), whereas  $\text{Fe}^{3+}$  commonly exists as 6-coordinate octahedral.<sup>43</sup> The consequences of inherent acidity and the subsequent hard-soft factors are known by the Irving-Williams' series and oxygen chelates.<sup>44</sup>

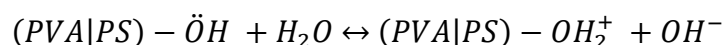


**Scheme 2:** Metal - ligand coordination phenomenon in the hydrogel network structure

The Irving-Williams' series of increasing stability of Ni and Cu is a measure of inherent acidity of the metal. Generally, if the ligand is hard (lone-pair electrons reside on the highly electronegative elements like oxygen) then it will favor the hard metals (the harder species like

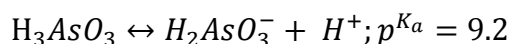
early transition metal ions which contain few d-electrons) to form the stable chelate.<sup>8</sup> Consequently, the materials containing ligands of oxygen-donating atoms such as  $-\ddot{O}-H$  functional group containing ligand prefer  $Fe^{3+}$  and  $Mn^{2+}$  ions, which have a few d-electrons than other metals, though there is an exception observed for  $Cr^{3+}$ . Allowing for ionic radii the above order is also showing consistency. However, softer species such as  $Cu^{2+}$  (which is of high d-electron) will come later to the ligand containing oxygen atoms to make the chelate. The observed exception is for  $Pb^{2+}$  and that may be due to the presence of different series of transition elements. However, all of the other metals laid on the first transition series. The facts, here is the performance of the chelating functionalized hydrogels to  $Fe^{3+}$  or other heavy metals is the most significant influence of oxidation state and atomic radii of the metals, stability constant and structure of chelates. The metal with the higher oxidation state is related to the shrinkage of size, leading to the increase of the charge on metal ion and the tendency of pulling the ligands in closer. Therefore, the prepared chelating functionalized hydrogels showed maximum selectivity towards  $Fe^{3+}$ .

**Fig. 5(b)** shows the arsenic species removal efficiency of PVA and PVA/polysaccharides blend hydrogels from aqueous solution. The free hydroxyl group ( $-\ddot{O}-H$ ) in PVA and polysaccharides exists in equilibrium with the protonated hydroxyl group in aqueous solution.



At neutral pH the hydroxyl groups ( $-\ddot{O}-H$ ) of PVA gels 'are mostly protonated (as  $-OH_2^+$ ) and the protonated groups are coexisting with the ordinary hydroxyl ( $-\ddot{O}-H$ ) groups also. On the other hand, the inorganic form of arsenic i.e., arsenite ( $As^{3+}$ ) is the most naturally abundant

element that exists in natural water of more than 70 countries of the world and in aqueous solution this arsenite species governed by:<sup>45</sup>



At neutral condition, this available species may coexist as electrically uncharged and charged species such as  $\text{H}_3\text{AsO}_3$  and  $\text{H}_2\text{AsO}_3^-$  which may prefer by the ordinary and protonated hydroxyl groups of the adsorbent gel, respectively.<sup>46</sup> The charged species of As ( $\text{H}_2\text{AsO}_3^-$ ) and protonated hydroxyl ( $-\text{OH}_2^+$ ) group of the gel may attach through electrostatic attraction<sup>47</sup> and the electrically neutral species ( $\text{H}_3\text{AsO}_3$ ) may interact with the ordinary hydroxyl ( $-\ddot{\text{O}}-\text{H}$ ) groups of the gel by following the Vander Waals attraction.

### 3.7. Re-use of the hydrogel chelates

To develop the viable adsorbent material to be used in any chelation system, the prepared hydrogels must be reusable with satisfactory removal performance in the environmental applications. Hence, the desorption performance of the  $\text{As}^{3+}$  species from the chelated hydrogels materials has been investigated. The result is summarized in Table 4, in the form of desorption ratio ( $D_r$ , %) and it was measured for 3 consecutive absorption/desorption cycles. The scopes of re-use for the prepared PVA/PS chelating functionalized hydrogels have been investigated and the results have been shown in **Table 4**. The results indicate that these materials could be easily regenerated. The desorption performances of the chelated hydrogels is around 90% in most cases even after three cycles.

**Table 4:** Desorption performances of chelated hydrogels

<i>D<sub>r</sub></i> (%) of Fe <sup>3+</sup>			
Cycle No.	1	2	3
PVA	92±3.26	91±1.63	90±1.81
PVA/MS	93±2.44	88±0.82	85±0.90
PVA/RP	92±2.21	89±2.86	89±1.84
PVA/WF	92±1.64	90±1.22	85±1.31
PVA/CS	91±2.86	90±1.42	88±1.35

<i>D<sub>r</sub></i> (%) of As <sup>3+</sup>			
Cycle No.	1	2	3
PVA	95±1.39	94±1.43	94±0.79
PVA/MS	93±1.30	91±1.72	91±1.23
PVA/RP	94±1.24	91±1.60	89±2.84
PVA/WF	94±2.16	92±0.49	89±0.84
PVA/CS	95±1.63	93±0.57	88±1.48

#### 4. Conclusion

In the present study, radiation grafted polyvinyl alcohol and polyvinyl alcohol /polysaccharides (blend) hydrogels were synthesized by  $\gamma$ -ray irradiation technique. The prepared materials are having a good gel fraction, high degree of swelling and very good adsorption performances for As<sup>3+</sup> and some heavy metals adsorption in comparison with other adsorbents reported in literature. The experimental data of water absorption follow Fickian

diffusion with maximum adsorption capacity 686% for polyvinyl alcohol /Corn Starch hydrogel. The chelating hydrogels exhibit sorption capacity of some heavy metals. Among the chelating materials, the hydrogel treated with corn starch prefer  $\text{Fe}^{3+}$  with the maximum absorption performance 37075 mg/kg, and almost all of the hydrogels showed low absorption tendency toward the  $\text{Pb}^{2+}$ . The developed hydrogels demonstrated a good arsenic removal performances and the maximum uptake 22112 mg/kg for the same hydrogel. These materials can be used up to 3 times with a high desorption rate (~90%). Basic medium (2M, sodium hydroxide) can be used for elution of the absorbed  $\text{As}^{3+}$  by exchanging the negatively charged species of arsenic whereas the heavy metal ions are eluted by using the hydrochloric acid solution. According to the results, 1 kg gels can remove heavy metal from about 400–200 L. Thus synthesized hydrogel materials are a good candidate for effective removal of arsenic and heavy metals from aqueous medium for the application in water treatment process and also potentially used for other applications of hydrogel.

## Acknowledgements

Authors would like to express their special thanks to Dr. Feroza Akhtar, Director of the Institute of Nuclear Science and Technology, Atomic Energy Research Establishment, Savar, Dhaka and A.K.M. Moshiul Alam, Senior Scientific Officer of the same institute for their mentionable support to do the work. Authors are thankful to Professor Matsuura Takeshi, Industrial Membrane Research Institute, University of Ottawa, Canada, for his valuable suggestion on the Manuscript. They would also like to acknowledge the University Malaysia Pahang, Malaysia for giving the financial support under the grant GRS110322 and M.N.K. Chowdhury to complete the work.

## References

1. W. W. A. Programme and UN-Water, *Water in a changing world*, Earthscan, 2009.
2. N. N. N. A. Rahman, M. Shahadat, C. A. Won and F. M. Omar, *RSC Advances*, 2014, **4**, 58156-58163.
3. N. Sahiner, O. Ozay, N. Aktas, D. A. Blake and V. T. John, *Desalination*, 2011, **279**, 344-352.
4. G. B. B. Varadwaj, S. Rana, K. Parida and B. B. Nayak, *Journal of Materials Chemistry A*, 2014, **2**, 7526-7534.
5. X. Wang, W. Liu, J. Tian, Z. Zhao, P. Hao, X. Kang, Y. Sang and H. Liu, *Journal of Materials Chemistry A*, 2014, **2**, 2599-2608.
6. R. K. Sharma, M. Agrawal and F. Marshall, *Ecotoxicology and environmental safety*, 2007, **66**, 258-266.
7. S. Huang, L. Gu, N. Zhu, K. Feng, H. Yuan, Z. Lou, Y. Li and A. Shan, *Green Chemistry*, 2014, **16**, 2696-2705.
8. M. Chowdhury, M. Khan, M. Mina, M. Beg, M. R. Khan and A. Alam, *Radiation Physics and Chemistry*, 2012, **81**, 1606-1611.
9. F. Peng, T. Luo and Y. Yuan, *New Journal of Chemistry*, 2014, **38**, 4427-4433.
10. R. Lozano, *Journal of Cleaner Production*, 2008, **16**, 1838-1846.
11. R. Lozano and D. Huisingh, *Journal of Cleaner Production*, 2011, **19**, 99-107.
12. W. Leitner, *Green Chemistry*, 2011, **13**, 1379-1379.
13. L. Li, H. Duan, X. Wang and C. Luo, *New Journal of Chemistry*, 2014, **38**, 6008-6016.
14. M. I. Litter, M. E. Morgada and J. Bundschuh, *Environmental Pollution*, 2010, **158**, 1105-1118.
15. H. S. Park, Y. C. Lee, B. G. Choi, W. H. Hong and J. W. Yang, *ChemSusChem*, 2008, **1**, 356-362.
16. T. A. Vu, G. H. Le, C. D. Dao, L. Q. Dang, K. T. Nguyen, Q. K. Nguyen, P. T. Dang, H. T. Tran, Q. T. Duong and T. V. Nguyen, *RSC Advances*, 2015, **5**, 5261-5268.
17. A. Bhatnagar and M. Sillanpää, *Advances in Colloid and Interface Science*, 2009, **152**, 26-38.
18. D. Li, X. Zhang, G. P. Simon and H. Wang, *Water research*, 2013, **47**, 209-215.
19. Y. Gao, Z. Wei, F. Li, Z. M. Yang, Y. M. Chen, M. Zrinyi and Y. Osada, *Green Chemistry*, 2014, **16**, 1255-1261.
20. P. Chakraborty, B. Roy, P. Bairi and A. K. Nandi, *Journal of Materials Chemistry*, 2012, **22**, 20291-20298.
21. C. Shen, Y. Shen, Y. Wen, H. Wang and W. Liu, *Water research*, 2011, **45**, 5200-5210.
22. M.-M. Titirici, A. Thomas and M. Antonietti, *Journal of Materials Chemistry*, 2007, **17**, 3412-3418.
23. J.-Y. Tseng, C.-Y. Chang, Y.-H. Chen, C.-F. Chang and P.-C. Chiang, *Colloids and Surfaces A: Physicochemical and Engineering Aspects*, 2007, **295**, 209-216.
24. M. Iravani, S. Tangestaninejad, M. Habibi and V. Mirkhani, *Journal of the Iranian Chemical Society*, 2010, **7**, 791-798.



25. M. K. Othman, F. A. Al-Qadri and F. A. Al-Yusufy, *Spectrochimica Acta Part A: Molecular and Biomolecular Spectroscopy*, 2011, **78**, 1342-1348.
26. J. C. Igwe, A. Abia and C. Ibeh, *International Journal of Environmental Science & Technology*, 2008, **5**, 83-92.
27. N. Ünlü and M. Ersoz, *Separation and Purification Technology*, 2007, **52**, 461-469.
28. H. Yirikoglu and M. Gülfen, *Separation science and technology*, 2008, **43**, 376-388.
29. M. Chowdhury, A. Alam, N. Dafader, M. Haque, F. Akhtar, M. Ahmed, H. Rashid and R. Begum, *Bio-medical materials and engineering*, 2006, **16**, 223-228.
30. M. Zhai, F. Yoshii, T. Kume and K. Hashim, *Carbohydrate polymers*, 2002, **50**, 295-303.
31. V. Vilay, M. Mariatti, R. Mat Taib and M. Todo, *Composites science and technology*, 2008, **68**, 631-638.
32. R. Kizil, J. Irudayaraj and K. Seetharaman, *Journal of agricultural and food chemistry*, 2002, **50**, 3912-3918.
33. M. Chowdhury, M. Mina, M. Beg and M. R. Khan, *Polymer bulletin*, 2013, **70**, 3103-3113.
34. M. Chowdhury, M. Beg, M. Khan, M. Mina and A. Ismail, *Colloid and Polymer Science*, 2014, 1-10.
35. P. Deeyai, M. Suphantharika, R. Wongsagonsup and S. Dangtip, *Chinese Physics Letters*, 2013, **30**, 018103.
36. A. T. Tu, J. Lee and F. P. Milanovich, *Carbohydrate Research*, 1979, **76**, 239-244.
37. Z. Maolin, H. Hongfei, F. Yoshii and K. Makuuchi, *Radiation Physics and Chemistry*, 2000, **57**, 459-464.
38. O. Güven, M. Şen, E. Karadağ and D. Saraydın, *Radiation Physics and Chemistry*, 1999, **56**, 381-386.
39. P. J. Flory, *Principles of polymer chemistry*, Cornell University Press, 1953.
40. A. Singh, S. Narvi, P. Dutta and N. Pandey, *Bulletin of Materials Science*, 2006, **29**, 233-238.
41. M. Mariatti, M. Nasir and H. Ismail, *Polymer testing*, 2001, **20**, 179-189.
42. S. Das, A. Saha, P. Choudhury, R. Basak, B. Mitra, T. Todd, S. Lang and R. Rowell, *Journal of applied polymer science*, 2000, **76**, 1652-1661.
43. H. A. El-Rehim, E. Hegazy and A. E.-H. Ali, *Reactive and Functional Polymers*, 2000, **43**, 105-116.
44. H. Irving and R. Williams, *J. Chem. Soc.*, 1953, 3192-3210.
45. B. E. Reed, R. Vaughan and L. Jiang, *Journal of Environmental Engineering*, 2000, **126**, 869-873.
46. V. M. Boddu, K. Abburi, J. L. Talbott, E. D. Smith and R. Haasch, *Water research*, 2008, **42**, 633-642.
47. Y. Gao, K.-H. Lee, M. Oshima and S. MOTOMIZU, *Analytical sciences*, 2000, **16**, 1303-1308.

**FIGURE CAPTIONS**

**Fig. 1:** Gel fraction ( $G_f$ ) of hydrogels with absorbed dose

**Fig. 2:** FTIR spectra of (a) polysaccharides and (b) their graft materials with PVA

**Fig.3:** Degree of swelling ( $D_s$ ) of different hydrogels

**Fig.4:** Water absorption performances of different hydrogels

**Fig.5:** Removal of heavy metal and arsenic by hydrogels

**TABLE CAPTIONS**

**Table 1:** Band assignments for FTIR spectra of polysaccharides

**Table 2:** Diffusion coefficient and moisture contents of hydrogels

**Table 3:** Microbial densities found in the prepared hydrogels

**Table 4:** Desorption performances of chelated hydrogels